Catalysis Letters 23 (1994) 13–24

X-ray photoelectron spectroscopic study of the oxidation and reduction of a cerium(III) oxide/cerium foil substrate

Dale A. Creaser [1], Philip G. Harrison

Department of Chemistry, University of Nottingham, University Park, Nottingham NG7 2RD, UK

M.A. Morris and B.A. Wolfindale

ICI Chemicals and Polymers, Katalco RTE, PO Box 1, Belasis Avenue, Billingham, Cleveland TS23 1LB, UK

Received 29 December 1992; accepted 11 August 1993

X-ray photoelectron spectroscopy has been used to examine the nature of the oxide overlayers on a passivated cerium metal foil as a function of a variety of oxidation and reduction treatments. Oxidation of a clean uncontaminated cerium(III) oxide surface is facile at room temperature and produces non-stoichiometric ceria (CeO_{2-x}) at oxygen doses as low as 10 L. At higher doses the overlayer thickens, and after a dose of 160 L the layer depth exceeds the Ce 3d photoelectron attenuation distance of about 20 Å. High pressure treatment of the foil in oxygen (0.5 bar at RT and 473 K) produces CeO_2 in a high degree of crystallographic order such that O 1s photoelectron intensities are increased above that expected from a randomly oriented powder. An attempt to reduce the CeO_2 layer formed by controlled oxidation with CO (633 K, 14 h, 0.6 bar) results in the formation of a carbonated surface layer. Results following attempts to reoxidise this layer are discussed.

Keywords: Cerium oxide, oxidation/reduction; XPS cerium

1. Introduction

Cerium oxide has attracted both academic and industrial interest in recent years due to its use as a catalytic material and also because of its electrical and magnetic properties. Ceria is widely used both as a catalyst support and as an active catalytic material. The most widespread application of ceria in catalysts is probably in the catalytic converter in automobiles for the removal of CO, hydrocarbons, and NO_x.

[1] Present address: ICI Chemicals and Polymers, Research & Technology, Analytical and Physical Sciences Group, PO Box 8, The Heath, Runcorn, Cheshire WA7 4QD, UK.

Doped with lanthanide cations, ceria has found application as a hydrocarbon oxidation catalyst. Of particular interest is the effective oxidation state of the cerium ion in processing conditions or in cerias doped with alternative metal atoms. Although many X-ray photoelectron spectroscopy (XPS) data on this type of system are available in the literature, they have generally been limited since the oxide powders examined suffer considerably from sample charging induced by the photoelectron process. We have experienced similar problems in studies of the oxidation and reduction of ceria using in situ gas treatments using XPS as a quantitative surface analysis probe. In order to alleviate this problem, we have carried out XPS studies on an earthed oxidised cerium metal foil.

There are few detailed studies on the oxidation of the 4f elements using photoelectron spectroscopy. Some examples exist for the oxidations of La [2–5], Gd [6,7], Sm [5], Tb [5] and Yb [7], and in each case the passivating layer is found to be the sesquioxide. The majority of investigations employed the lanthanide 3d and the O 1s core level photoelectron spectra as the spectroscopic probes. It was found that the transition from the metal spin–orbit doublet ($3d_{3/2}$ and $3d_{5/2}$) spectrum to the oxide spectrum, where the spin–orbit pairs were accompanied by large satellites to lower binding energy, allowed a quantitative determination of oxidation along with estimate of oxide depth. The simple O 1s spectra generally consisted of features attributable to oxide (O^{2-}) and peroxide (O_2^{2-}) [4] (or physisorbed oxygen [8]) species. The surface oxidation of cerium metal has been studied by few authors. In the earliest study [9], the nature of the oxide on the surface could not be established. Later studies by Platau and coworkers [8] employed both XPS and UPS and established the passive layer to be insulating Ce_2O_3 with an estimated thickness of 10 Å. However, it was suggested that high oxygen exposure had little further effect. Praline and co-workers [11] oxidised clean cerium foil at sub-ambient temperatures (120–300 K) and found that oxygen adsorption initially forms cerium(IV) oxide. The thickness of the layer is greater than 24 Å after only a 20 L dose both at 120 and 300 K. They also ascribe oxygen features as being due to oxide in Ce_2O_3 and CeO_2 after only 50 L oxygen dose. Similar conclusions are arrived at by Sarma, Hegde and Rao [5].

This present work describes the oxidation and reduction of an oxidised ceria surface upon cerium metal. The oxidations involve low gas doses (10 L) to comparatively extreme conditions of 1 bar at 473 K. Further, the interpretation of the Ce 3d photoelectron spectra following our spectral assignments [1] enables an accurate and reliable determination of spin–orbit coupling constant data.

2. Experimental

X-ray photoelectron spectra were recorded using a VSW multi-technique surface science instrument fitted with an in situ high pressure reaction vessel. The exciting radiation employed was Al $K\alpha_{1,2}$ (1486.6 eV) at 180 W. The hemispherical

analyser was operated in constant energy mode at a pass energy of 50 eV. All spectra, unless otherwise stated, were acquired at 298 K and a minimum background pressure of $<5 \times 10^{-8}$ Torr. Under these conditions, the sample remains uncontaminated for up to 1 h. Since the sample is earthed the binding energies quoted are unreferenced. Analysis of the raw spectra was carried out within the spectra acquisition software.

A sample of cerium foil of thickness 0.25 mm (Aldrich Chemicals) was cut to a square of dimensions 25×25 mm^2. The specimen was cleaned with very fine grade emery cloth. Tantalum wire was threaded through holes at the periphery of the foil and was attached to copper rods which formed part of the sample manipulation mechanism and were attached to a series of three high precision micrometer position adjusters. The copper rods also allowed the temperature of the foil to be controlled to within 2–5 K, by resistively heating the tantalum wire. A chromel–alumel thermocouple junction was made at the edge of the foil. Oxygen (BDH, 99.999%) was admitted to the UHV chamber by back-filling through a variable leak valve. Low pressure dosings are quoted in langmuirs ($1\ \mathrm{L} = 10^{-6}$ Torr s). Higher pressures of oxygen and carbon monoxide were admitted to a high pressure reaction vessel. This vessel was wound up to enclose the sample and was protected from the UHV conditions by means of a knife edge/copper gasket joint. After treatment the vessel was evacuated before the sample was re-exposed to the UHV chamber.

The cerium foil sample, after mechanical and chemical cleaning treatments was subjected to Ar^+ ion bombardment at 10 kV, 1.8 mA and 607 K for 8.25 h and then annealing in UHV at 673 K for 1 h to restore surface order.

3. Results and discussion

3.1. THE SAMPLE ON INTRODUCTION

The Ce 3d spectrum shown in fig. 1 (a) illustrates the surface of the metal foil prior to the Ar^+ bombardment. This spectrum is indicative of a non-stoichiometric cerium(IV) oxide layer. Recent work by us [1] has enabled each of the component peaks of the three regions in the Ce 3d spectrum to be assigned to features due to Ce^{4+} and Ce^{3+} cations. Indeed, oxygen deficient non-stoichiometry of cerium(IV) oxide (CeO_{2-x}) is accompanied by the presence of oxygen vacancies and Ce^{3+} cations according to eq. (1):

$$O_O^X \rightarrow V_O^{**} + 2e' + \tfrac{1}{2}O_2(g)\,, \tag{1}$$

where, in Kroger–Vink notation, O_O^X is an O^{2-} anion in a normal lattice site within the fluorite structure, V_O^{**} is an anion vacancy and e′ is a defect which is known to exist as a small polaron, i.e. it associates with a Ce^{4+} cation, effectively reducing it to Ce^{3+}.

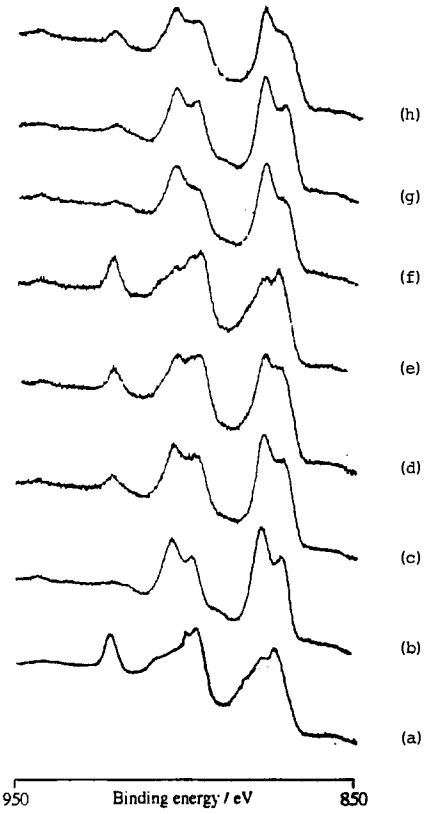

Fig. 1. Ce 3d photoelectron spectra obtained for the (a) passivated cerium foil, (b) after Ar^+ ion bombardment at 673 K for 8.25 h, and after (c) 15, (d) 60, and (e) 1000 L O_2 dose, (f) CO reduction (0.6 bar, 633 K, 14 h), (g) annealing a 823 K for 2 min in UHV and (h) 800 L O_2 dose.

3.2. ARGON ION "PROCESSING" OF THE SURFACE

After the ion bombardment and the annealing, the Ce 3d spectrum shows a dramatic change in appearance (fig. 1 (b)). The spectrum comprises a spin–orbit pair of doublets, which is fully consistent with Ce_2O_3 as reported previously [5,8,11] and confirmed by our own recent analyses of Ce^{3+} compounds. The feature to the high binding energy side of each doublet is the $3d^94f^1$ core–hole photoemission final state from the Ce^{3+} cation. The satellite at lower binding energy is a shake-down feature due to the ligand (O 2p) to metal (Ce 4f) charge transfer initiated by the photoionisation process [1,12].

The cleaning of the surface, i.e. the removal of the non-stoichiometric ceria overlayer to leave a cerium(III) oxide substrate, can be quantitatively followed by the calculation of O^{2-}/Ce, the atomic ratio, and the subsequent calculation of x in CeO_x. This is achieved by a well defined route. Firstly, values of peak area per scan were found by subjecting each spectral envelope in the Ce 3d and O 1s spectra to a

Shirley-type background subtraction routine [13]. Normalised peak areas can then be established. The values of peak area per scan for the O 1s and Ce 3d regions are then ratioed to find a qualitative surface composition. Taking this ratio, along with other parameters such as Schofield photoionisation cross sections [14], analyser geometry, instrument functions and escape depths, enabled quantitative atomic ratios to be calculated. The in-house software developed by Morris is described in detail elsewhere [15]. The quoted values of x in CeO_x for the surface before and after Ar^+ ion bombardment are 1.96 and 1.46. The data quoted are estimated to be accurate to at least 10% of the absolute values. This corroborates evidence from simple examination of the 3d core spectra where the reduction from ceria (where $x = 2$ for stoichiometric ceria) to cerium(III) oxide (where $x = 1.5$) was observed. It should also be stated that the O/Ce stoichiometry and the form of the spectrum indicate that the analyte analysed by XPS is almost pure Ce_2O_3.

3.3. OXIDATION OF Ce_2O_3

Curves (c)–(e) of fig. 1 illustrate the Ce 3d spectra for the surface after a preliminary oxidation at oxygen doses of 15, 60 and 1000 L. Indeed, it is obvious by inspection, that the cerium(III) oxide substrate has been further oxidised with growth of a ceria overlayer. The calculated values of x for the three dosing experiments are 1.69, 1.83 and 2.10. It is thus quite reasonable to expect the surface to be fully oxidised after the 1000 L oxygen dose.

In order to define each spectral feature within the envelopes of the Ce 3d spectrum, the convention adopted is that used by Burroughs and co-workers [2] and also in our earlier work [1], and is shown in fig. 2. In the case of the Ce 3d spectrum of cerium(IV) oxide, the features labelled as t* and t are due to the $3d^9 4f^1$ photoemission final state from the Ce^{3+} cation. The satellites s* and s are caused by the facilitation of the ligand (O 2p) to metal (Ce 4f) charge transfer (LMCT) by the primary photoionisation process and is a shakedown feature. This results in a final

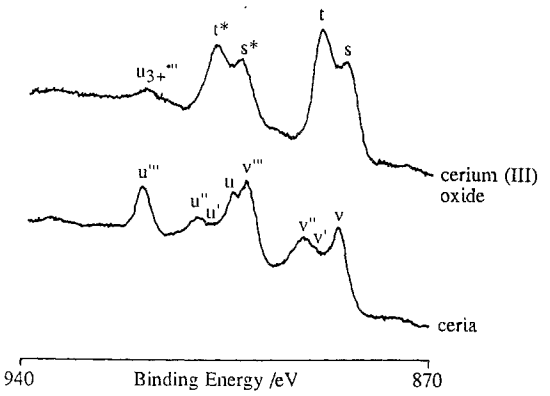

Fig. 2. Nomenclature used in the definition of the features observed in the Ce 3d photoelectron spectra of cerium(III) oxide and ceria.

state approximating to $3d^9 4f^2$. The two regions are split by spin–orbit coupling, with the $3d_{3/2}$ components lying at higher binding energy. The photoelectron spectrum for the cerium(IV) oxide is somewhat more complex. There exist a total of eight individual peak components which comprise two sets of four. Those labelled u are the $3d_{3/2}$ spin–orbit features whilst their $3d_{5/2}$ partners are labelled v. Primary photoionisation gives rise to the final state $3d^9 4f^{10}$ (Ce^{5+}), and to the peaks u''' and v'''. In much the same way as the shakedown is facilitated in cerium(III) oxide, so it also occurs here. Two LMCTs are possible: the single LMCT resulting in a final state approximating to $3d^9 4f^1$ (u'' and v''), and a second LMCT which accesses a final state approximating to $3d^9 4f^2$ (u and v). Peaks designated u' and v' are thought to be due to the photoemission of the Ce^{3+} cation, i.e. the $3d^9 4f^1$ photoemission final state.

Due to the gradual oxidation under the low gas exposures used throughout this work, an exact transition between the spectrum for Ce_2O_3 and that of ceria is often very difficult to establish and many spectra are a sum of envelopes from a mixture of 3+ and 4+ states. In the quoting of binding energy data, therefore, if the features marked u and v are resolvable from the raw spectrum, they are designated (4+), otherwise the t and s nomenclature (3+) is used.

3.4. REDUCTION OF CeO_2 BY CO

After this regime of preliminary oxidation, the material was subjected to carbon monoxide reduction (0.6 bar, 633 K, 14 h). Fig. 1 (f) shows the Ce 3d photoelectron spectrum after this reduction. By inspection, the surface overlayer of ceria has been reduced and the substrate appears to be solely that of cerium(III) oxide. After this reduction the specimen was annealed in UHV at 823 K for 2 min (fig. 1 (g)). Surprisingly, however, the reduction caused an increase in the O 1s/Ce 3d and C 1s/Ce 3d peak area ratios. After the reduction, the O 1s/Ce 3d peak area ratio rose from 0.113 (the value after the 1000 L dose of oxygen) to 0.128 and the C 1s/Ce 3d peak area ratio rose from an unmeasurable value (i.e. an undetectable C 1s signal) to 0.057.

This apparent anomaly can be rationalised with the aid of the O 1s photoelectron spectra shown in fig. 3, curves (a)–(d). Fig. 3 (a) shows the O 1s spectrum after 1000 L oxygen dose. The spectrum comprises two peaks at binding energies (unreferenced) of 530.8 eV, ascribed to the oxide entity, and 533.1 eV, which is most likely due to residual surface peroxide groups [4]. That the latter high energy peak is due to surface hydroxyl may be excluded since, in separate experiment where hydroxylated surfaces were deliberately formed, the peak due to OH^- occurs around 531.5 eV. Corroboration of this could be obtained from valence band data with He II UPS. Curves (b) and (c) of fig. 3 illustrate the changes observed after CO reduction and annealing. The shoulder around 533 eV increases in intensity many-fold. This is attributed to surface carbonate species formed by the oxidative chemisorption of CO on the substrate surface. That the peroxide, assigned as such

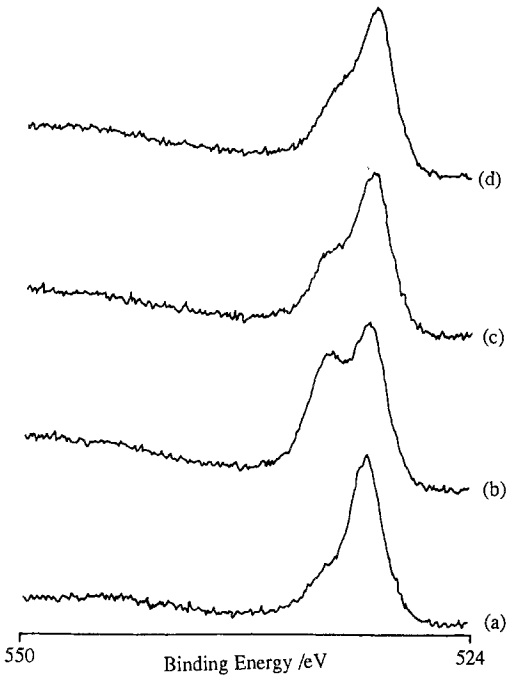

Fig. 3. O 1s photoelectron spectra observed after (a) 1000 L O_2 dose on clean Ce_2O_3, (b) after CO reduction (0.6 bar, 633 K, 14 h), (c) after annealing at 823 K for 2 min in UHV and (d) after 800 L O_2 dose on the contaminated substrate.

due to the absence of any resolvable C 1s signal, and carbonate peaks are coincident is fortuitous. The decrease in the intensity of the carbonate peak after annealing is accompanied by a reduction in the C 1s/Ce 3d peak area ratio to 0.050. The O 1s/Ce 3d area ratio falls to 0.101, showing that following carbonate decomposition some Ce is observed in the 3+ state (see the ratio of the oxidised surface). Thus, CO treatment yields a Ce(III) carbonate surface layer.

The effect of the surface carbonate under these conditions is to dramatically affect the facile oxidation of the Ce_2O_3/Ce substrate. This is exemplified by figs. 1 (h) and 3 (d). The Ce 3d photoelectron spectrum of the surface after an 800 L oxygen dose reveals little of the structure attributable to the Ce^{4+} cation. Fig. 3 (d) also illustrates the resilience during high oxygen exposures of the carbonate peak. It thus appears that the surface is poisoned towards further oxidation by the surface carbonation. The O 1s/Ce 3d and C 1s/Ce 3d peak area ratios change to 0.113 and 0.053, respectively, after the 800 L oxygen dosing. Hence, the carbonate species are stable under these conditions. Dosing for 800 L at 573 K reduces the carbonation somewhat, with a C 1s/Ce 3d ratio reduction to 0.041.

Curve-fitting of the O 1s spectrum into its two component peaks, i.e. oxide and carbonate, enables the calculation of the area due to the oxide component alone and hence the value of x in CeO_x. The value of x for the surface material after CO

reduction is 1.71 which is unchanged after annealing. Oxygen dosing (800 L) at ambient temperature increases the value of x to 1.80, whilst further oxygen treatment at 573 K results in a further increase to 2.02 illustrating that the Ce^{3+} associated with the carbonate can be slowly oxidised.

3.5. DETAILED OXIDATION STUDIES

Before any careful oxidation experiments were performed on this contaminated surface, the surface was cleaned by Ar^+ ion bombardment at 633 K until the C 1s signal was not detectable (4 h). After this, the value of x was observed to reduce to 1.45, i.e. Ce_2O_3, and the Ce 3d spectrum (fig. 4 (a)), was of the expected appearance.

Curves (b)–(j) of fig. 4 show the Ce 3d photoelectron spectra obtained after progressive oxygen treatments of 10, 20, 40, 80, 160, 320, and 640 L dosings (figs. 4 (b)–(h)), 1 bar pressure for 64 h (fig. 4 (i)) and 0.5 bar pressure at 473 K for 10 min (fig. 4 (j)). The changes observed in the Ce 3d photoelectron spectrum with oxidation are those expected from our previous work [1]. The bands u‴ and u″, along with v‴ and v″, are the most obvious spectral features to be seen to increase since

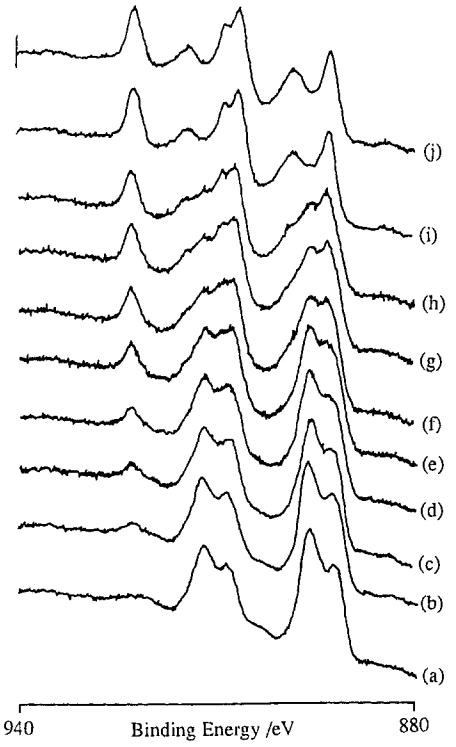

Fig. 4. Ce 3d photoelectron spectra of (a) clean Ce_2O_3 after Ar^+ ion bombardment at 633 K for 4 h and (b)–(h) after O_2 dosings of 10, 20, 40, 80, 160, 320 and 640 L, (i) oxidation with 1 bar pressure oxygen at RT for 64 h, and (j) oxygen treatment (0.5 bar) at 473 K for 10 min.

they are due to the Ce^{4+} cation only. The bands t* and t, the photoionisation final state from the Ce^{3+} cation, reduce in intensity with oxidation as would be expected. Peaks s* and s, which would be expected to be coincident with the u and v features in the ceria spectrum, are seen to become more intense with oxidation, i.e. with the increase in abundance of Ce^{4+} species. After extensive oxidation, the Ce 3d photoelectron spectrum is void of any resolvable Ce^{3+} features and exhibits the usual (4+) twin set of three peaks (fig. 4 curves (i) and (j)).

Obviously, as the surface is oxidised, the O 1s/Ce 3d peak area ratio is expected to increase. This is manifested by an increase in the calculated value of x in CeO_x after the O 1s spectrum has been peak fitted to enable the use of the oxide component only. Table 1 details the value of x as a function of oxygen dose.

The apparent almost saturation after a dose of approximately 160 L is most probably due to the ceria overlayer becoming thicker than the photoelectron attenuation length (which for Ce 3d photoelectrons is about 20 Å [16]) rather than the cessation of the oxidation process. It is expected that there is still a slow bulk oxidation occurring via grain boundary diffusion etc., which is confirmed at very high oxygen doses.

Individual binding energies for the component peaks have not been presented here. Nevertheless the average binding energies for the component peaks in the u and v and t and s notation are listed in table 2. The u'''_{3+} feature is a peak which is comparable with that observed in the ceria spectrum (u'''). It most likely suggests that the cerium(III) oxide is actually slightly oxidised. The other features associated with the Ce^{4+} cation are masked by the intense t and s peaks. It is interesting to note that in the Ce 3d photoelectron spectrum of non-stoichiometric cerium(IV) oxide, the u' and v' peaks are assigned to the Ce^{3+} cation only. Indeed, the position of these features should match exactly those of the t* and t features in the Ce 3d photoelectron spectrum of Ce_2O_3, which is borne out from the data in table 2. The one electron shakedown process occurring in the cerium(III) oxide spectrum (s* and s) results in a final state which approximates to that giving rise to u and v in the ceria spectrum. Once again, within the errors of peak measurement of the poorly resolved shoulders, the positions of s* and s appear coincident with those of u and v, respectively.

The magnitude of the spin–orbit coupling is simply the energy difference between a feature in the $3d_{3/2}$ ionisation and its corresponding partner in the $3d_{5/2}$ ionisation. Energy differences calculated from the values in table 2 are shown in

Table 1
Change in value of x in CeO_x as a function of oxygen dose

O_2 dose (L)	x in CeO_x	O_2 dose (L)	x in CeO_x
0	1.45	80	1.84
10	1.65	160	2.03
20	1.73	320	2.08
40	1.75	640	2.09

Table 2
Mean binding energy positions (eV) for all features observed in the oxidation and reduction studies (see text)

Peak	u'''_{3+}	t*	s*	t	s			
mean BE	920.0	907.4	903.1	888.7	885.0			
Peak	u'''	u''	u'	u	v'''	v''	v'	v
mean BE	920.0	910.3	907.3	904.0	902.0	891.9	888.5	885.6

table 3. The average value of the $3d_{3/2}-3d_{5/2}$ spin–orbit coupling is 18.4 eV in good agreement with the value quoted by Borroughs and co-workers (18.7 eV) [12]. The shakedown energies, i.e. u'''–u'' and u'''–u', are 9.7 (10.1) and 16.0 (16.4) eV, respectively, the values in parentheses being those for the equivalent $3d_{3/2}$ processes.

Prolonged treatment of the substrate with oxygen, giving rise to the Ce 3d spectra in fig. 4 (i) and (j), yields a value of x in CeO_x of 2.42 after exposure to 1 bar oxygen pressure for 64 h at 298 K, and 2.47 after exposure to 0.5 bar oxygen pressure at 473 K for 10 min. Due to the inability of the cerium atom to be further oxidised from its tetravalent state, these values appear anomalous. However, Caro et al. [17] have shown how lanthanide metal foils may be oxidised to provide a stable sesquioxide phase of predetermined and constant crystal behaviour with respect to the metal substrate. It can be imagined here that the surface, after A^+ ion bombardment, is rough. After oxidation, however, the growth of the oxide layer is controlled to produce an array of sesquioxide crystals, all of which are crystallographically aligned. Further, more drastic, oxidation will enable the ceria to grow on these crystals. Generally, when the metal foil is oxidised, C-type sesquioxide is produced with the {111} planes parallel to the metal surface. This crystal type is essentially a fluorite lattice with 25% oxygen vacancies. If such is the case for cerium(III) oxide, then it can be seen that this arrangement will enable an ordered growth of CeO_2, either by the filling of the vacancies of the C-type sesquioxide lattice, or more likely by its use as a template for the nucleation of the ceria fluorite type phase. The result is a long range ordering of cerium(IV) oxide crystals. Thus the observed high values of x may be rationalised as a result of this ordering. Exposed planes of the fluorite lattice are the {100}, {110} and {111} in increasing

Table 3
Spin–orbit splitting parameters for the features observed in the Ce 3d photoelectron spectra of cerium(III) oxide and ceria

Transition	Energy splitting (eV)	Transition	Energy splitting (eV)
u'''–v'''	18.1	u–v	18.4
u''–v''	18.4	t*–t	18.7
u'–v'	18.8	s*–s	18.1

proportion of the total. Since only the {100} and {111} planes are composed entirely of oxygen atoms it would appear that the ceria crystals have an orientation such that much of the CeO_2 surface layers are terminated by these planes, and this enhances O 1s intensities relative to the Ce 3d. The very high crystallographic order will also ensure that photoelectron diffraction occurs and may have been measured as an increase in the O 1s photoelectron flux.

4. Summary

This study has examined the nature of the oxides formed on cerium foil and has found that the passive overlayer of cerium(III) oxide is readily oxidised to cerium(IV) oxide at low oxygen doses. This facile oxidation is slowed by carbonation of the cerium(III) oxide prior to oxygen dosing. Extensive oxidation of cerium(III) oxide produces ceria (CeO_2) in a high degree of crystallographic order. This study has also enabled the calculation of spin–orbit splitting and shakedown energy parameters to compliment our earlier study [1].

Acknowledgement

One of us (DAC) would like to thank ICI plc and SERC for funding through the CASE scheme. The authors thank M. Fowles and W.C. Mackrodt for stimulating discussions. The ICI Strategic Research Funding Scheme is acknowledged for project support.

References

[1] D.A. Creaser, P.G. Harrison, B.A. Wolfindale and M.A. Morris, in: *Catalysis and Surface Characterisation*, eds. T.J. Dines, C.A. Rochester and J. Thompson (Royal Society of Chemistry, Cambridge, 1992) p. 261.
[2] Y. Baer and G. Busch, Phys. Rev. Lett. 31 (1973) 35.
[3] L. Schlapbach, Solid State Commun. 33 (1981) 117.
[4] S.L. Qui, C.L. Lin, J. Chen and M. Slrongin, Phys. Rev. B 41 (1990) 7467.
[5] D.D. Sarma, M.S. Hegde and C.N.R. Rao, J. Chem. Soc. Faraday Trans. II 77 (1981) 1509.
[6] P.D. Schulze and E.L. Hardegree, J. Phys. Chem. 93 (1989) 5254.
[7] M. Ayyoob and D.D. Sarma, Ind. J. Chem. 22A (1983) 731.
[8] A. Platau, L.I. Johansson, A.L. Hagstrom, S.-E. Karlsson and S.B.M. Hagstrom, Surf. Sci. 63 (1977) 153.
[9] C.R. Helms and W.E. Spicer, Appl. Phys. Lett. 21 (1972) 237.
[10] A. Platau and S.E. Karlsson, Phys. Rev. B 18 (1978) 3820.
[11] G. Praline, B.E. Koel, R.L. Hance, H.-I. Lee and J.M. White, J. Electron. Spectry. Relat. Phenom. 21 (1980) 17.
[12] P. Burroughs, A. Hamnett, A.F. Orchard and G. Thornton, J. Chem. Soc. Dalton Trans. (1976) 1686.

[13] D.A. Shirley, Adv. Chem. Phys. 23 (1973) 85.
[14] J.H. Scofield, J. Electron Spectry. Relat. Phenom. 8 (1976) 129.
[15] M.A. Morris, ICI C&P Internal Report No. IC 10454.
[16] M.P. Seah and W.A. Dench, Surf. Interf. Anal. 1 (1979) 2.
[17] P.E. Caro, G. Schiffmacher, C. Boulesterix, Ch. Loier and R. Portier, in: *Defects and Transport in Oxides*, eds. M.S. Seltzer and R.I. Jaffee (Plenum Press, New York, 1974) 521.